

# AIAA'88

AMERICAN INSTITUTE OF  
AERONAUTICS AND ASTRONAUTICS  
AIAA 88- 307

~~MISSING PAGE~~

**AIAA-88-0307**

## **The 3-D Flowfield in a Supersonic Shock Boundary Layer Corner Interaction**

Paul Batcho, John Sullivan, Purdue  
University, West Lafayette, IN

ENGINEERING LIBRARY  
TECHNICAL REPORTS

## **AIAA 26th Aerospace Sciences Meeting**

January 11-14, 1988/Reno, Nevada

THE 3-D FLOWFIELD IN A SUPERSONIC SHOCK  
BOUNDARY LAYER CORNER INTERACTION

Paul Batcho<sup>1</sup>  
John Sullivan<sup>2</sup>  
Purdue University  
West Lafayette, Indiana

ABSTRACT

An experimental investigation of the corner interaction of a two-dimensional compression ramp with both turbulent floor and sidewall boundary layers was carried out in the Purdue University high-Reynolds number Mach 2.56 blow down wind tunnel. Detailed floor and sidewall surface flow visualization along with flowfield visualization are presented to qualitatively define the flow structure. The constraints imposed by the rules of topology along with experimental observations and laws of fluid dynamics indicate the presence of two distinct interactions. One vortical system is established by the glancing shock sidewall interaction and travels downstream along the sidewall. Another vortical system, which originates from the separation bubble at the ramp's beginning, travels along the ramp surface and then turns downstream near the sidewalls forming a horseshoe vortex. The experimental observations and conclusions presented in this study will be an aid in the construction of computational codes and zonal methodologies being used in current high speed research efforts.

1.) INTRODUCTION

There has been a considerable effort paid to the complex flow phenomenon of shock boundary layer interactions. Reviews of the subject [1]-[3] have shown that the qualitative structures of the two dimensional phenomenon are well understood although much of the detailed fluid dynamics has yet to be resolved. Much of the effort in the past has focused on understanding the two-dimensional problem and thus giving a firm basis to analyze the 3-D phenomenon. Except for recent investigations there has been little research into either the three-dimensional or the inherently unsteady nature of the interactions.

Studies of swept compression ramps and glancing shock interactions have been carried out in an effort to study the three-dimensional influences [4]-[5]. However the increasing interest in supersonic and hypersonic flight has brought with it a need for an efficient supersonic inlet capable of operation over a wide range of mach numbers. These advanced inlets may consist of boundary layers comprising up to fifty percent of the inlet flow. The flowfield will consist of several shock boundary layer interactions with the presence of wall and floor boundary layers, see Figure 1. An understanding of the complex flow structures that exist in shock boundary interactions with large 3-D disturbances is therefore needed.

The highly three-dimensional surface patterns on the floor of a shock boundary layer interaction have been noted by several authors [1], [9]-[12]. The studies show the considerable influence of the sidewall boundary layers on the structure of the separated flows. However, the above studies have been for incident shock impingement where the ramp interaction was believed to be of a similar nature. There has been little attempt in the past to discuss the topology of the interactions which may yield considerable insight into the interactions. The present investigation uses the constraints imposed by the rules of topology along with experimental observations and the laws of fluid dynamics to obtain an understanding of the fundamental mechanisms which comprise such an interaction.

Current computational efforts [4] have attempted to model the flow structure with the use of zonal methodology and the three dimensional parabolic Navier-Stokes equations. For interactions with a significant separation region present there has been considerable discrepancies between experimental measurements and computational results. However, the zonal methodology relies heavily on a prior knowledge of the flowfield which is not sufficiently understood. Flow visualization is obtained in the present study in an attempt to piece together the complex flowfield. Visualization of the flowfield, wall and floor surfaces were made for this purpose.

1 Currently Research Assistant, Princeton University, Student Member AIAA

2 Professor, Aeronautics and Astronautics, Member AIAA

Studies into the unsteady nature of the shock boundary layer interactions have been carried out and indicate an elevated region of unsteady behavior at the separation line of the ramp interaction [13]. From the behavior of oil induced at the surface the present investigation has observed increased unsteadiness at the separation line. There was also indications of shock oscillations from the schlieren photography. The gross or mean structure of the flowfield is assumed to be unaffected by the unsteadiness. By the above assumption the use of topological arguments, which apply to an instantaneous field, are applied to the mean flowfield. However no further studies were carried out in the present investigation concerning the unsteady behavior of the interaction.

The flow studied in this investigation has a fully turbulent incoming boundary layer at a Mach number of 2.56 and two-dimensional wedge angles of 10, 15, and 20 degrees. The interaction at the corner of the ramp and the sidewall is investigated where the span to boundary layer thickness ratio was approximately 10.

## 2) DESCRIPTION OF EXPERIMENT

### Facility

The experimental investigation was carried out in the Purdue University high-Reynolds number 1.75 by 2.21 inch blow down wind tunnel; a sketch of the facility appears in Figure 2. The compression ramp test model was mounted on the floor of the test section which is 13 inches downstream of the nozzle throat. The present tests were performed at a free-stream mach number of 2.56, a stagnation pressure of 2.9 atm., and a stagnation temperature of 524 R (291 K). The tunnel is approximately adiabatic yielding an incoming boundary layer thickness of .18 inches and Reynolds number/in. =  $7.2 \times 10^6$ , ( $Re_\delta = 1.3 \times 10^7$ ).

### Test Models and Instrumentation

The 10 and 15 degree compression ramp models were sized to insure that the pressure distribution along the centerline had reached the two-dimensional inviscid value. The 20 degree ramp did not yield the inviscid pressure rise however a separation region of five boundary layers in length enabled very detailed surface flow visualization. The centerline was tapped with 17 pressure taps along the floor and was sampled with a scanning valve and pressure transducer system. The static pressure distributions are believed to be accurate to within  $\pm 4\%$ . Data acquisition and reduction was performed by a digital computer.

### Boundary Layer

The undisturbed floor boundary layer was measured with a pitot probe which had a .008 in. ID port for sampling. The measurements were taken in .01 in. increments yielding a Mach number profile presented in Figure 3. The velocity profile was obtained by assuming a constant total temperature across the boundary layer. The velocity profile is presented in Figure 4 and is compared to the 1/7 power law profile for turbulent incompressible flow. The comparison is consistent with results of other investigations for compressible turbulent boundary layers of the same nature [14]. Due to the tunnel geometry the wall and floor boundary layers are expected to be the same size.

### Surface Flow Visualization

Many techniques for surface flow visualization were used such as surface oil flows, applying discrete dots of paint, kerosene-lampblack mixtures (as proposed in [15]), LCD crystal visualization, and a line oil paint technique developed during the investigation. Oil paint is applied to the surface in

either discrete dots or a line. The shear forces would then spread the paint along the direction of surface streamlines. In order to preserve the results the surface was first covered with scotch tape; which could then be removed after the experiment. Different color paints were applied so that the behavior of distinct regions of the interaction could be identified. A 35 mm photograph was then taken of the wedge surface.

### Flow Field Visualization

A local vapor screen method [15] was used to visualize the corner region of the ramp and sidewall. A volatile liquid is injected into the corner region through a .03 inch tap. The liquid is then vaporized by the flow generating a dense fog which can be seen and photographed under suitable lighting. For the conditions of the test section alcohol was found to yield the best results. The injection orifice was located 1/8 inches from the wall of .5 inches from the ramp. A 5mW helium-neon laser was used to illuminate the particles in the flow by producing a laser sheet in the crossflow plane (see Figure 5). Photography was performed by a video camera mounted at a slight angle to the side of the tunnel. The particles were lifted into the flowfield by the vortical fluid generated within the wall boundary layer at the separation line. The video picture was recorded by a VCR and then digitized and color enhanced by computer software. Flowfield visualization was only performed for the 15 degree wedge interaction.

The pumping system was naturally available due to the subatmospheric pressure present in the test section. A metering valve was connected to regulate the mass flow of liquid. Only a low flow rate was required to achieve the present results and the addition of more fluid did not increase the size of the vortical system visualized.

### Optical Flow Visualization

A color schlieren was used to photograph the shock system created by the compression ramp. The schlieren was also integrated with the wall surface visualization to find the location of the inviscid shock relative to the viscous effects at the wall.

## 3) PRESENTATION OF RESULTS

### Surface Interactions

A full span ramp is used to produce an interaction between the oblique shock wave generated by the ramp and incoming sidewall and floor boundary layers. The ramp surface visualization of the 15 and 20 degree interactions are presented in Figures 6 and 7. Detailed visualization was performed on the 20 degree wedge by several colors of oil paint to enhance the topological features of the surface. The centerline separation lengths were two and five times the incoming boundary layer thicknesses for the 15 and 20 degree ramps respectively. The pressure distribution along the centerline reaches its inviscid pressure at approximately five boundary layer thicknesses downstream of the ramp for the 15 degree interaction (see Figure 8). The 10 degree ramp yielded a separation length of 0.8 boundary layers and reached its inviscid pressure rise at approximately 4.5 boundary layers downstream of the ramp's corner. These results agree well with the results of Green [1], [16] at Mach 2.5 for incident shock impingement with wall effects and equivalent Reynolds number based on boundary layer thickness. The floor topological features of the 10 degree ramp interaction were observed to be similar to the 15 and 20 degree ramp interactions with corresponding smaller separation bubble length. Wall visualizations of the 10 and 15 degree ramp interactions are presented in Figures 9 and 10.

## Flowfield Visualization

The flowfield was visualized with a laser sheet at two locations along the 15 degree surface. The first was at the start of the ramp model and the second was at four boundary layers downstream from the corner. There was no substantial increase in the size or structure of the interaction visualized from the start of the ramp to the second location. The photographs indicate the presence of two vortical structures traveling down the surface of the ramp (see Figure 11). Surface visualizations indicate the presence of two regions of flow of opposite sense. The generation of a secondary flow of opposite sense (secondary vortex) by a larger vortical flow is common in a corner region. The influence of the primary vortical structure is approximately 2.5 boundary layers from the wall and the height of the structure is visualized to be equivalent to one boundary layer. This may indicate that the interaction is largely contained within the domain of the incoming boundary layers.

## 4) DISCUSSION OF RESULTS

### Surface Interaction

Figures 6 and 7 show the highly three-dimensional phenomenon that is present at the surface. A strong spiral node was present at the corner region of the separation line and was primarily contained within the length of the wall boundary layer. A series of point node to saddle connections were visualized along the reattachment line of the separation bubble. For the 15 and 20 degree interaction a distinct region where no oil paint from the central separation region was allowed to enter was observed in the small corner region of the ramp's surface and tunnel wall, as noted in Figure 7a. This behavior is an indication of the presence of a separatrix that separates two distinct regions of flow. The direction of shear lines in the small corner region was observed by examining the behavior of small oil paint dots placed there (see Figure 7b). The presence of the strong spiral node is an indication of the start of a vortical flow that travels along the glancing shock sidewall separation line. The small corner region directly adjacent to the separation bubble is an indication of a secondary separation. It is thought that the glancing shock interaction is the result of low momentum flow in the corner under the influence of a strong adverse pressure gradient. This overturning is expected to draw the low energy fluid into the flowfield via a vortical structure. This behavior has been observed by the studies of glancing shock interactions without the presence of a floor boundary layer [4]-[6]. For the 15 and 20 degree interactions a very tight convergence of skin-friction lines along the sidewall of separation is indicated.

The strong spiral node is centered at the converging skin-friction lines as illustrated by the composite of the wall and floor surface visualizations of the 15 degree ramp (see Figure 12). The line of separation is an indication of the inviscid shock's upstream influence through the boundary layer. From the simultaneous use of the color schlieren and surface oil visualizations the location of the inviscid shock was indicated relative to the surface shear lines and is given in Figure 13 and 14. The flow near the wall is shown to be moving upward and parallel to the separation line rather than parallel to the ramp's surface. The appearance of S-shaped lines of shear, on the sidewall, emanating from the line of attachment near the wedge surface have also been noted in the glancing shock interactions with no floor boundary layer present [6]. Studies of the corner flow interactions of two wedges have also indicated surface wall visualization of a similar nature [17]. As the vortical flow on the sidewall travels downstream its influence increases and it begins to lose its identity as indicated by the lessening curvature to the shear lines. The 10 degree ramp

interaction did not indicate the presence of a tight coalescence of shear lines along the glancing shock interaction. However, a strong spiral node on the floor corner region was still present.

On the floor of the interaction all lines of shear upstream and in the separation bubble appear to be entering the strong spiral node in the corner. The separatrix indicated by the bubble's separation line shows this behavior in Figure 7c. The region of flow in the small corner region which is behind the ramp separation bubble is contained between a separation line on the floor and a reattachment line on the sidewall. The flowfield visualization indicates this to be the result of a small secondary vortex traveling downstream. The shear lines emanating from the dominate point node on the reattachment line, of the separation bubble, either curve back towards the sidewall or align parallel to the centerline. The lines that curve back towards the sidewall indicate the influence of the vortical flow traveling along the ramp's surface. The lines which asymptote to a line parallel to the centerline indicate that the vortical system reaches an equilibrium influence in the spanwise direction as it travels downstream. For both the 10 and 15 degree ramp interactions the equilibrium influence was found to be 2.5 boundary layers from the sidewall. The 10 and 15 degree interaction reached their equilibrium influences at approximately 4 and 1.5 boundary layers downstream respectively.

In order to describe the entire surface interaction the topological rules imposed on a continuous vector field are applied to the surface shear stress [18]. The skin-friction lines on a simply connected tunnel, without gaps, that extends to infinity both downstream and upstream must satisfy the condition that the sum of the nodes equals the sum of the saddles. Figure 15 is a sketch of the proposed topology of the surface shear stress that satisfy all constraints of topology and experimental observations. The series of saddle to point nodes along the reattachment line of the floor interaction gives the indication of a highly three-dimensional interaction. The saddle to saddle connection along the plane of symmetry seems to be observed by many researchers in shock boundary layer interactions where a strong plane of symmetry is imposed on the flow. Possible alternative arguments are micro-structures which are not resolved by the experiment or separatrices from the saddles which just miss each other. The latter is not possible if a plane of symmetry exists and the authors find no indication of micro-structures existing in the interaction. It is believed that based on the existence of a strong plane of symmetry created by vortical flows traveling down the ramps surface a saddle to saddle connection does exist along the centerline.

### Flowfield Interaction

The experimental observations indicate the presence of vortical flow along the sidewall which originates at the strong spiral node on the floor and is similar to those observed by published glancing shock studies. The vapor screen and floor surface visualizations also indicate the presence of a vortical flow traveling downstream on the ramp's surface. It is believed that these two vortical flows are distinct from each other. The separation bubble is a region of vorticity that must satisfy the solenoidal properties of its vector field. The lines of vorticity must either end at a surface, close on themselves or extend to infinity. There is no indication of the separation bubble closing on itself or ending on the surface. This leads to the conclusion that the separation bubble is extending to infinity in the form of a horseshoe vortex traveling downstream along the corner of the ramp's surface. The vapor screen is visualizing the floor separation bubble traveling downstream along the corner of the ramp and sidewall. Using the constraints of topology on the flowfield crossflow plane and plane of symmetry, Figure 16 is arrived at. The crossflow plane represents the direction of the flowfield vectors tangent to the plane pictured. The origin of the vortical flow that travels along the

sidewall is visualized particularly well by the large floor spiral node of Figure 7d. The interaction presented was arrived at by satisfying the flowfield and surface visualizations along with the topological and fluid dynamic constraints imposed on a continuum. The sidewall and floor interactions are pictured to be separated by a separatrix which enters a saddle point in the flowfield and also separates the primary and secondary flows of the floor interaction.

Throughout the present discussion the vortical flow is not referred to as a vortex. This is due to the experimental and computational observations of a vortical sheet being present in the interactions of swept ramp models [19]. It is not clear as to which type of vortical flow is present, vortex or sheet, in the corner region of the current investigation. Although the flowfield visualizations do indicate the presence of a core region in the primary vortical structure. Although concerns about the use of the term "separation" in 3-D interaction have been expressed [19], the present study uses the topological methods and definitions as outlined by Tobak and Peake [18].

The use of the present flowfield visualization is a useful tool in describing the flowfield structure. The vapor particles present, however, are only visualizing the flow structures that easily carry them. Because of this limitation the complete interaction, such as the flow near the side wall, is not visualized.

The presence of a corner shock wave, which would separate the vortical fluid and inviscid free-stream, is also expected to exist. This was not visualized by the present investigation due to the limitations of the current facilities.

## 5) CONCLUSION

The present study of the corner glancing shock boundary layer interaction at a Mach number of 2.56 has used surface and flowfield visualization to obtain a qualitative flow structure of a 2-D wedge intersecting a planar sidewall. The interaction was characterized by moderate to strong interactions which gave a range of centerline separation lengths of 0.8 to 5 times the incoming boundary layer thickness.

Evidence of three distinct vortical flow structures was presented. One vortical system originates from the separation bubble at the ramp's beginning and turns downstream near the sidewalls forming a horse shoe vortex. The glancing shock induces boundary layer separation on the side wall generating a second vortex structure which originates from a spiral node on the floor and travels up the side wall. A third vortical structure is present in juncture of the ramp and sidewall.

The presence of a saddle to saddle connection was also visualized along the centerline. The study does support the existence of a saddle to saddle connection when a "strong" plane of symmetry exists.

The experimental observations and conclusions presented in this study are expected to be a valuable aid in construction of computational codes and zonal methodologies being used in current research efforts.

## 6) REFERENCES

- [1] Green, J.E., 1970, "Interactions Between Shock Waves and Turbulent Boundary Layers," *Prog. in Aerospace Science*, 11:235-340.
- [2] Hankey, W.L., Jr., Holden, M.S.; "Two-Dimensional Shock Wave Boundary Layer Interactions in High Speed Flows", AGARDograph #203.
- [3] Adamson, T.C., Messiter, A.F., "Analysis of Two-Dimensional Interactions between Shock Waves and Boundary Layers," *Ann. Rev. Fluid Mech.* 1980, 12:103-138.
- [4] Anderson, B.H., "Three-Dimensional Viscous Design Methodology of Supersonic Inlet Systems for Advanced Technology Aircraft", *Prog. Astro&Aero Vol. 102*, pp 431-480.
- [5] Horstman, C.C., Hung, C.M., "Computation of Three-Dimensional Turbulent Separated Flows at Supersonic Speeds," *AIAA Paper 79-0002*.
- [6] Settles, G. and Dolling, D., "Swept Shock Wave Boundary-Layer Interactions" In *tactical Missile Aerodynamics*, AIAA Progress in Astronautics and Aeronautics Series, 1986, Vol. 104, pp. 297-379.
- [7] Teng, H.Y., Settles, G.S., "Cylindrical and Conical Upstream Influence Regimes of 3D Shock/Turbulent Boundary Layer Interactions," *AIAA-82-0987*.
- [8] Settles, G.S., Bogdonoff, S.M., "Scaling of two and Three-Dimensional Shock/Turbulent Boundary Layer Interactions at Compression Corners," *AIAA-81-0334*, Vol. 20, No. 6.
- [9] Hingst, W.R., Jurkovich, M., "Flow Visualization of Shock Boundary Layer Interactions," *AIAA Paper N82-32675*.
- [10] Reda, D.C., Murphy, J.D., "Shock Wave Turbulent Boundary Layer Interactions in Rectangular Channels," *AIAA Paper No. 72-715*.
- [11] Reda, D.C., Murphy, J.D., "Shock Wave Turbulent Boundary Layer Interactions in Rectangular Channels, Part 2: The Influence of Sidewall Boundary Layers on Incipient Separation and Scale of the Interaction," *AIAA Paper No. 73-234*.
- [12] Voisinet, R.L.P., "An Experimental Investigation of the Compressible Turbulent Boundary Layer Separation Induced by a Continuous Flow Compression," *AGARD CP168*, 1975.
- [13] Dolling, D.S., Murphy, M.T., "Unsteadiness of the Separation Shock Wave Structure in a Supersonic Compression Ramp Flowfield," *AIAA Journal*, Vol. 12, No. 12, pp. 1628-1634.
- [14] Law, C.H., "Two-Dimensional Compression Corner and Planar Shock Wave Interactions with a Supersonic Turbulent Boundary Layer," *ARL TR75-0157*, June 1975.
- [15] Settles, G.S., Teng, H.Y., "Flow Visualization Methods for Separated Three-Dimensional Shock Wave/Turbulent Boundary Layer Interaction," *AIAA Journal*, March 1983, Vol. 21, pp. 390-397.
- [16] Green, J.E., "Reflexion of an Oblique Shock Wave by a Turbulent Boundary Layer," *J.Fluid Mech.*, 1970, Vol. 40, pp. 81-95.

[17] Watson, R.D., Weinstein, L.M., "A Study of Hypersonic Corner Flow Interactions," AIAA Paper 70-227.

[18] Tobak, M., Peake, D.J., "Topology of Two-Dimensional and Three-Dimensional Separated Flows," AIAA Paper 79-1480, July 1979.

[19] Bogdonoff, S.M., "Observation of the Three-Dimensional "Separation" in Shock Wave Turbulent Boundary Layer Interactions," Proceedings of the IUTAM Symposium on Turbulent Shear-Layer/Shock Wave Interactions, edited by J. Delery, Palaiseau, France, September 1985, to be published by Springer-Verlag.

ADVANCED INTEGRATED HIGH SPEED INLET SYSTEM  
Mach 5.0 Hypersonic Inlet

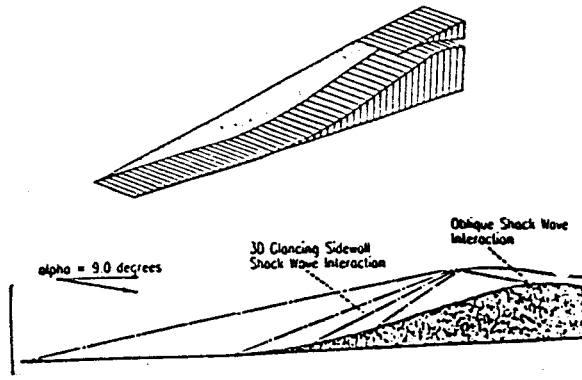


Fig. 1 Shock System in a Mach 5 Hypersonic Inlet (taken from [4]).

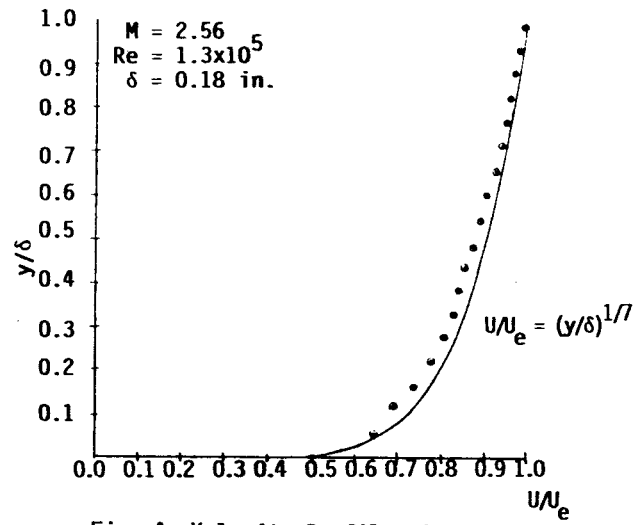


Fig. 4 Velocity Profile of the Undisturbed Tunnel Floor Boundary Layer

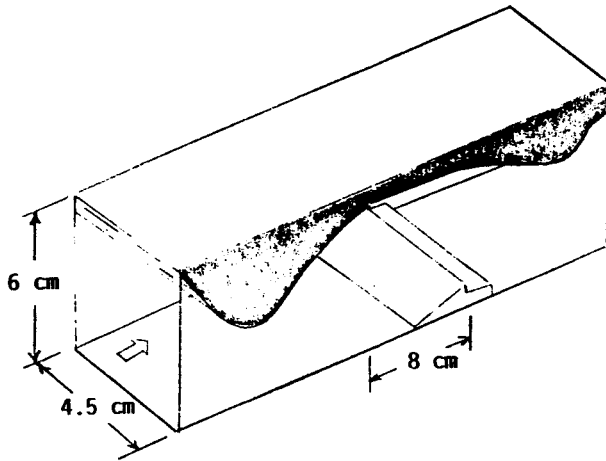


Fig. 2 Purdue University's High Reynolds Number Supersonic Tunnel, Aerospace Sciences Laboratory,  $M = 2.56$ ,  $Re_\delta = 1.3 \times 10^5$

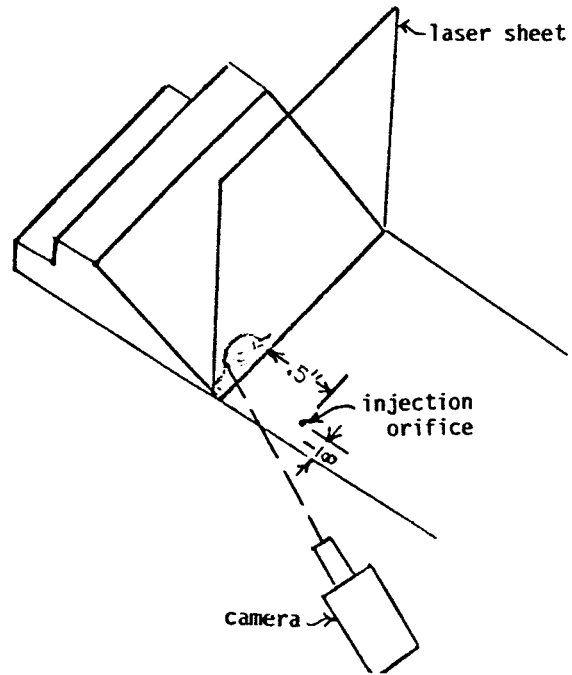


Fig. 5 Sketch of Flowfield Visualization Technique

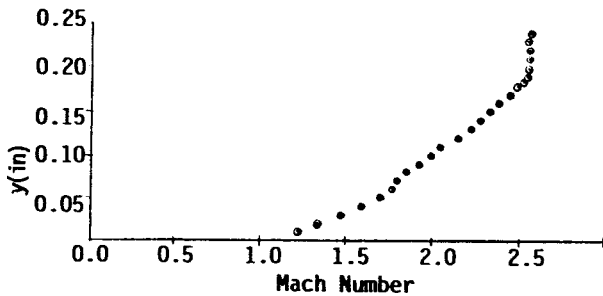


Fig. 3 Mach Number Profile in the Undisturbed Tunnel Floor Boundary Layer



Fig. 6a Flow Visualization

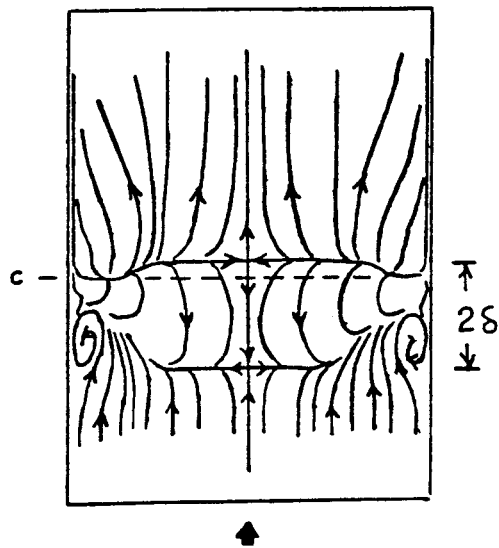


Fig. 6b Sketch of Interaction

Fig. 6 Floor Surface Visualization of 15° Ramp Interaction  $M = 2.56$  (top view)

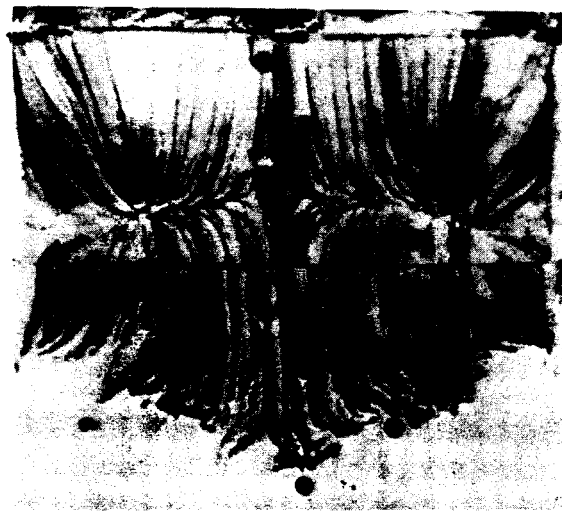


Fig. 7a Visualization From a Line of Oil Paint Placed Along The Reattachment Line

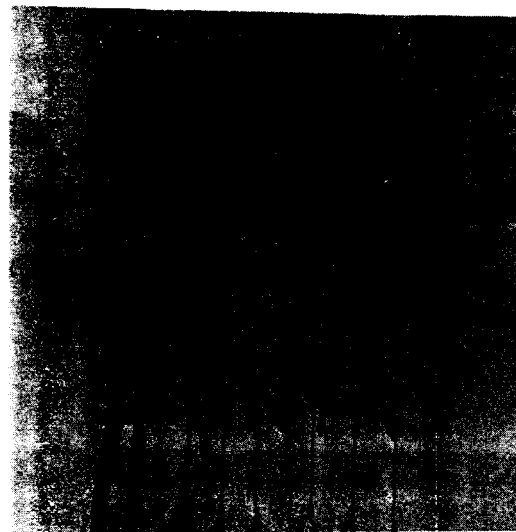


Fig. 7b Illustration of Secondary vs Primary Flow Directions

Fig. 7 Surface Oil Paint Visualization of 20° Ramp Interaction





Fig. 7c Illustration of Shear Lines Directed into the Spiral Node

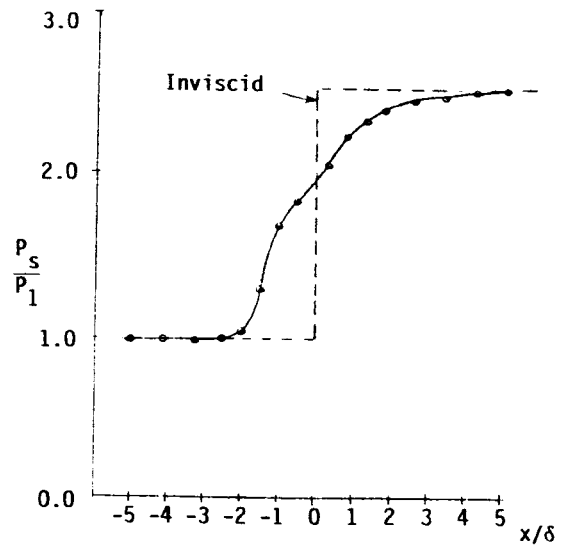


Fig. 8 Centerline Pressure Distribution for the 15° Ramp Interaction



Fig. 7d Illustration of Spiral Node and Closing Streamline on the Surface



Fig. 9a Line Paint Visualization

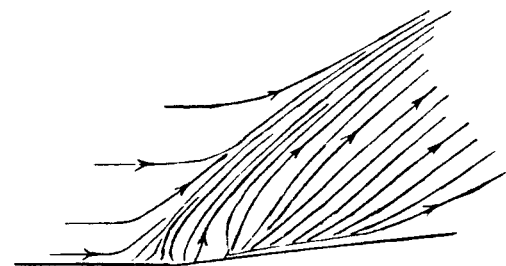


Fig. 9b Sketch of Shear Lines

Fig. 9 Wall Surface Visualization of the 10° Ramp Interaction, M = 2.56

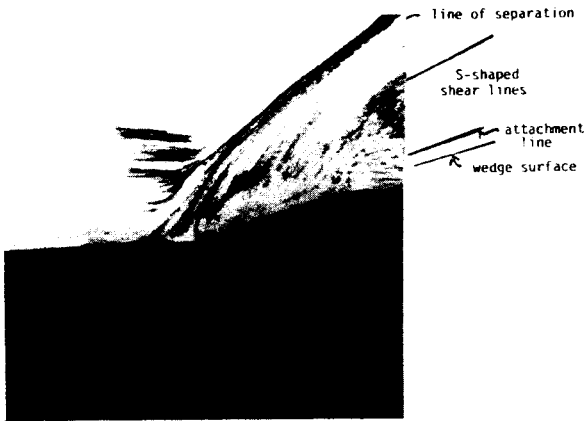


Fig. 10a Line Paint Visualization



Fig. 12 Composite of Wall and Floor Surface Visualization for the 15° Ramp Interaction

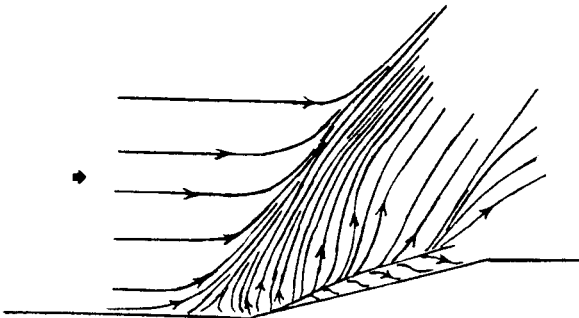


Fig. 10b Sketch of Shear Lines

Fig. 10 Wall Surface Visualization of 15° Ramp Interaction  
M = 2.56



Fig. 11 Flowfield Visualization Obtained From the 15° Ramp Interaction

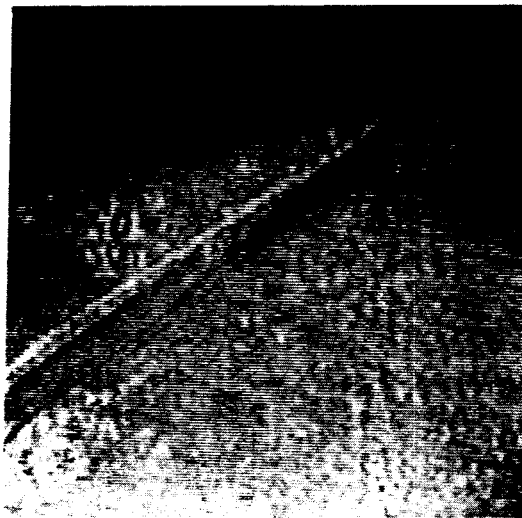


Fig. 13a Schlieren Photograph

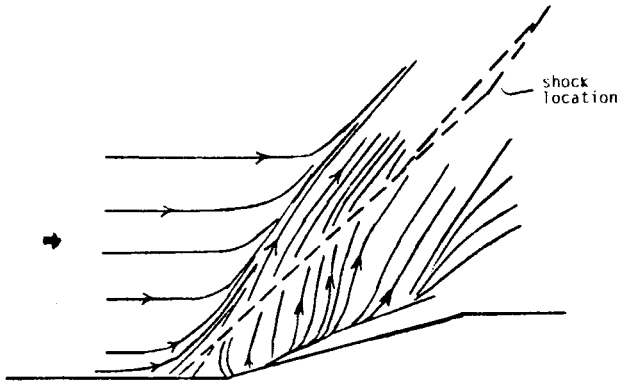


Fig. 13b Sketch of Observations

Fig. 13 The Location of the Inviscid Shock Relative to the Wall Line of Separation for the 15° Ramp Interaction

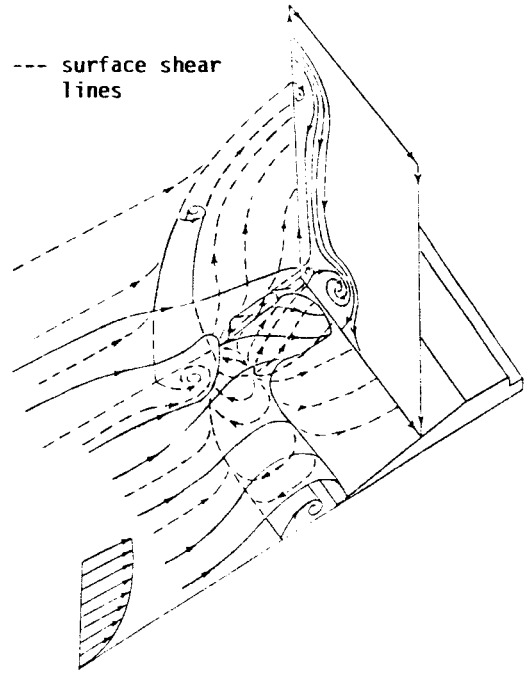


Fig. 16 Sketch of Qualitative Feature of the Interaction

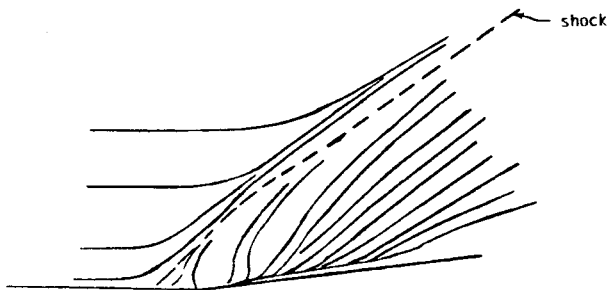


Fig. 14 Sketch of Observed Inviscid Shock Location for the 10° Ramp Interaction  $M = 2.56$

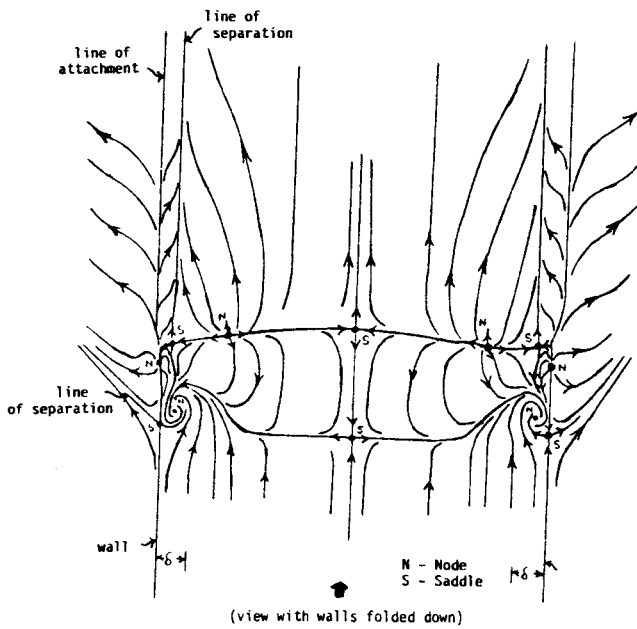


Fig. 15 Sketch of Observed Topology of Surface Shear Lines